

Comparison of photoacoustic, diffuse reflectance, attenuated total reflectance and transmission infrared spectroscopy for the study of biochars

Sylvia Pasieczna-Patkowska^{1*}, Jarosław Madej²

¹Faculty of Chemistry, Maria Curie Skłodowska University, 3 Maria Curie-Skłodowska Sq., 20-031 Lublin, Poland

²Lublin University of Technology, Department of Geotechnics, Faculty of Civil Engineering and Architecture, 40 Nadbystrzycka Str., 20-618 Lublin, Poland

*Corresponding author: e-mail: sylvia.pasieczna@poczta.umcs.lublin.pl

Four infrared spectroscopic techniques – photoacoustic (PAS), diffuse reflectance (DRS), attenuated total reflectance (ATR) and transmission (TS) – were evaluated for the qualitative analysis of the biochar obtained from willow feedstock during pyrolysis. Increase in pyrolysis temperature resulted in more aromatic and carbonaceous structure of biochars. These changes could easily be detected from Fourier transform infrared (FT-IR) spectral differences. The comparison of the spectra obtained by the four FT-IR techniques allowed to conclude that there are differences in the spectra acquired using different IR technique caused by different signal acquisition. PAS and ATR were the best techniques used in order to obtain spectra with smooth and sharp peaks, in contrast to TS, where bands were less-separated. DRS turned out to be the weakest of all techniques, due to poor spectral quality and poor separation of the bands.

Keywords: biochar; surface analysis; infrared spectroscopy.

INTRODUCTION

Biochar is a carbon-rich solid material obtained from the thermochemical conversion of biomass in a zero-oxygen or an oxygen-limited environment. Biochar can be used as a product itself or as an ingredient within a blended product, with a range of applications as an agent for improvement of soil fertility and plant growth, improved resource use efficiency, remediation and/or protection against particular environmental pollution. A wide range of organic materials are suitable as raw material for thermal processing, i.e. agricultural and wood biomass to any available agricultural, industrial wastes (bark, husks, straw, seeds, peels, bagasse, nutshells, sawdust, wood shavings, animal beds, etc.) or municipal wastes. Chemical and physical characteristics of biochar can vary widely depending on the converted feedstock and the operating conditions of the pyrolysis process. Particular biochar's application strongly depends on its physical and chemical properties¹. As a result, biochar should be characterized and defined by its production process in addition to its specific chemical composition and solid structure².

In order to determine the physicochemical properties of biochars various methods are used, including: elemental analysis including Atomic Absorption Spectrometry (CHN and metals content analysis, respectively) and Inductively Coupled Plasma (ICP), specific surface area measurements (S_{BET}), pH and zeta potential measurements, acid-base titration (quantity of acidic and basic functional groups), cation exchange capacity (CEC) and electrical conductivity (EC) measurements, X-ray diffraction (determination of mineral content) and infrared spectroscopy.

The latter is one of the techniques that allows for a quick overview of the type of functional groups formed on the biochar surfaces during pyrolysis. It has been one of the most frequently used instrumental analysis methods and it is a powerful technique for investigating

molecular chemistry of biochars. FT-IR supplements the results obtained using other analytical methods.

A range of different infrared techniques, including photoacoustic spectroscopy (PAS), attenuated total reflectance (ATR), diffuse reflectance spectroscopy (DRS) and transmission spectroscopy (TS), can be utilized to characterize biochars. However, all aforementioned techniques have some disadvantages and limitations and the selection of the suitable technique is important in order to examine the surface of the biochar as precisely as possible. Analysis of biochars and other carbon materials with a very high carbon content, by transmission IR spectroscopy is extremely difficult due to the fact that such materials, being optically opaque, almost completely absorb incident IR radiation. Grinding and dilution in potassium bromide may cause the destruction of their structure. For this reason, analysis of these materials is performed mainly by using ATR, DRS and PAS techniques.

Traditional transmission technique, the oldest and most commonly used, is useful only to study a sample bulk, and the major problem is the interference of the water present in potassium bromide used for the pellets preparation. Moreover, removing water from already made pellets may introduce chemical changes in the carbon material sample. DRS, PAS and, to some extent, ATR are free from interference caused by the presence of water. PAS and ATR are so-called surface techniques which allow to distinguish the bulk of the sample from its surface^{3, 4}. PAS, ATR and DRS are called surface techniques, because signal is generated from a few micrometres of the surface and provide information about the chemical structure of the near-surface region. Surface sensitivity is $\sim 1\mu\text{m}$ for PAS, $\sim 10\text{\AA}$ for DRS and monolayer for ATR⁵. TS allows to see the bulk of the biochar. Additionally, DRS can analyze both bulk and surface, depending on the method of sample prepara-

tion (grinding with potassium bromide or analyzing the sample as is, respectively).

Infrared spectroscopy is rapid, relatively simple and efficient tool for biochar characterization, but interpretation of the IR spectra of carbons and biochars is rather complicated. This is due to the fact that each of the functional groups connected to the appearance of multiple bands in the IR spectrum may have contribution of many of the functional groups present on the surface of the sample.

All the aforementioned techniques (PAS, DRS, ATR, TS), to a greater or lower extent, have been used for analysis of surface functional groups of coals and biochars. ATR is now the most common sampling technique in FT-IR spectroscopy and it is widely used for identification of functional groups in biochars. ATR technique was used, i.e. for investigation of the influence of pyrolysis temperature on the physicochemical properties of biochars^{6–8}, the effect of the pyrolysis method on the physicochemical properties of biochars⁹, analysis of biochars prepared from various agricultural by-products^{10, 11} and characterization of biochars produced in oxygen-limited conditions¹². However, ATR has some disadvantages. IR spectrum obtained using this technique is not identical to the spectrum obtained by e.g. transmission method. ATR introduces relative shifts in band intensity (bands at long wavelengths appear relatively stronger than bands at short wavelength), which fortunately can be easily corrected mathematically. A more difficult problem is absolute shift in frequencies, which can result in a displacement of the peak maximum. This can lead to ambiguous interpretation of the ATR spectrum. Additionally, this technique suffers from a lack of a good contact between the sample and refractive ATR crystal what can lead to non-accurate results¹³. The transmission technique does not have these disadvantages but, as it was mentioned, suffers from the water interference. Spectral artefacts such as baseline shifts due to light scattering can be also found in transmission spectra of KBr pellet³. TS has been used to study biochars obtained from different feedstock and at different temperatures of pyrolysis^{14–18}, biochars derived from various agricultural residues¹⁹, mineralization of biochars²⁰ and effects of biochar addition on organic matter humification²¹.

In DRS, there is no linear relation between the reflected light intensity (band intensity) and concentration of the sample, in contrast to TS in which the band intensity is directly proportional to concentration. In diffuse reflectance technique particles size, homogeneity, and packing density of powdered samples play important role on the quality of IR spectrum. Since the diffusion coefficient strongly depends on sample preparation, thus the reflectance intensity is influenced by the sample preparation. The same sample may produce different spectra in different experiments. Raw DRS spectra appear different from its transmission analogue, but a Kubelka-Munk conversion can be applied to DRS spectrum to compensate for these differences. This technique can be non-destructive when the sample is measured directly, without prior grinding, however thus obtained spectra are frequently noisy, or destructive when the sample is grounded and mixed with KBr (but no compressing is needed) to reduce particle size and thus avoid light scattering by rough surfaces.

DRS technique has been used e.g. for the study of biochar obtained from dairy manure²².

The main advantage of photoacoustic spectroscopy is the fact that no elaborate sample preparation is required. This technique is non-destructive, it can be used in the analysis of materials which are difficult to homogenize, or the structure or the chemical composition change during grinding²³. Even samples with rough surfaces and strongly scattering infrared light can be easily measured, since the photoacoustic signal is proportional to the absorbed energy, not reflected as in the case of reflectance techniques. Although, PAS method has a poor signal-to-noise ratio, so longer data acquisition is required than using other three infrared techniques. This relatively young technique is increasingly used in the analysis of biochars^{21, 24–27}.

To the authors' best knowledge, there are no studies reporting comparison of TS, ATR, DRS and PAS using mid-FT-IR spectroscopy for detection of biochars functional groups, although biomass and biomass-derived materials have been studied by Gogna and Goacher (TS, ATR, DRS)²⁸ and Faix and Böttcher (TS, DRS)²⁹. Yang and Simms³ compared TS, DRS and PAS for the study of carbon fibers.

In this study three biochar samples from a willow feedstock were prepared in different temperatures (500, 600, 700°C) during pyrolysis. Four infrared spectroscopic techniques (PAS, DRS, ATR, TS) were used and compared in order to find the most suitable IR technique for biochar analysis. Thus, the purpose of this work was not strictly to examine the chemical composition of biochars, but to determine the suitability of various IR spectroscopy techniques to evaluate the quality differences between the spectra of examined biochars.

EXPERIMENTAL

Biochar production

Willow feedstock was cut by hand to small pieces, sieved over a 2mm sieve and the rest cut again until all the feedstock measured pieces <2 mm. Then feedstock was subjected to pyrolysis (50 g per run) in the sealed furnace of the design described in [30]. Biochar (BCW) was prepared at 500°C (BCW 500), 600°C (BCW 600) and 700°C (BCW 700). The furnace was heated at a rate of 25 K/min. An oxygen-free atmosphere during the process of pyrolysis was maintained by the constant flow of nitrogen, which was controlled with the mass flow controller (BETA-ERG, Poland). The nitrogen gas was dosed straight from the bottle and injected at a rate 630 ml N₂/min (at 298 K, 101.2 kPa). The gas outlet from the furnace was protected by a scrubber. The pyrolysis temperature was held for 4 h (slow pyrolysis). Three runs of pyrolysis were conducted for every sample. Each pyrolysis run resulted in one sample replicate. After each pyrolysis sample was homogenized and oven-dried at 40°C for 48 h. Subsequently, all samples were kept in sealed plastic bags and maintained at 4°C until they were used.

Analytical methods

The chemical properties of biochars were determined by standard methods. The pH was measured potentiometri-

cally in 1 M KCl after 24 h in the liquid/biochar ratio of 10. The amount of carbon, hydrogen and nitrogen were determined using CHN analyzer (Perkin–Elmer 2400). Ash content of biochars samples were determined by dry combustion at 760°C for 6 h³¹. The oxygen content in biochars was calculated from mass balance. To analyze the textural characteristics of materials, low-temperature (77.4 K) nitrogen adsorption–desorption isotherms were recorded using a Micromeritics ASAP 2405 N adsorption analyzer. The specific surface area S_{BET} was calculated according to the standard BET method³². In each case, three replicates were performed and the results are the average of these measurements while relative standard deviation is less than 6%.

Infrared spectroscopy instrumentation

The transmission (TS) and photoacoustic (PAS) spectra of the biochar samples were recorded by means of Bio-Rad Excalibur FT-IR 3000 MX spectrometer over the 3800–600 cm^{-1} range at room temperature, resolution 4 cm^{-1} and maximum source aperture. TS spectra were obtained using the KBr pellet method. The sample (~1 mg) was mixed and ground in an agate mortar with 300 mg of spectroscopically pure dry potassium bromide (48 h, 105°C) to a fine powder and then it was pressed to form a disk less than 1 mm thick. Data were collected at room temperature under air. Interferograms of 64 scans were averaged for each spectrum. PAS spectra were recorded using MTEC Model 300 photoacoustic cell. Dry helium was used to purge the PAS cell before data collection. The spectrum was normalized by computing the ratio of a sample spectrum to the spectrum of a MTEC carbon black standard. A stainless steel cup (diameter 10 mm) was filled with biochar sample (thickness <6 mm). Interferograms of 1024 scans were averaged for the spectrum, providing good signal-to-noise (S/N) ratio.

DRS and ATR spectra were recorded in the 3800–600 cm^{-1} range, resolution 4 cm^{-1} , at room temperature using Nicolet 6700 spectrometer. DRS spectra were obtained using Praying Mantis Diffuse Reflection Accessory (Harrick) and MCT detector. The biochar sample was placed in a metal container, without prior grinding. Interferograms of 256 scans were averaged for each spectrum. ATR spectra were recorded using Meridian Diamond ATR accessory (Harrick). Biochar samples were directly applied onto the diamond crystal, and close contact was made with the surface by a pressure tower. Interferograms of 256 scans were average for each spectrum. Dry potassium bromide (48h, 105°C) was used as a reference material to collect both DRS and ATR spectra. All DRS and ATR spectra were corrected for water vapour and carbon dioxide and ATR correction was applied. No smoothing functions were used for TS, DRS, ATR and PAS spectra.

All spectral measurements were performed at least in triplicate. The position of the bands in the spectra made with selected technique was identical for each sample, the spectra differed in the noise level resulting mainly from the presence of moisture.

The spectra presented in this work were obtained for samples dried for at least 72 h at 105°C. In all the cases, application of larger number of scans did not result in significant improvement in the quality of the spectra.

RESULTS AND DISCUSSION

Biochar characteristics

The physicochemical properties of the analysed biochars are presented in Table 1. All the biochars, regardless of temperature, were alkaline. The increase in pyrolysis temperature increased the pH of the biochars.

Increasing temperature of the pyrolysis process caused increase in carbon content from 75.18 wt.% for BCW 500 to 82, 38 wt.% for BCW 700 biochar. The hydrogen content decreased from 2.52 to 1.46 wt.% and oxygen content decreased from 11.65 to 8.85 wt.%. As temperature rose, H/C and O/C ratio decreased, implying that the biochars became more aromatic and carbonaceous¹⁶. This fact has the confirmation in the IR spectra of examined biochars, what will be discussed later.

Fourier transform infrared photoacoustic infrared spectroscopy (FT-IR/PAS)

The evolution of FT-IR/PAS spectra of biochars as a function of pyrolysis temperature is shown in Figure 1. For the purpose of better visibility, all spectra discussed further in this work were divided into two ranges: 3800–2400 cm^{-1} and 2000–600 cm^{-1} . Presented spectra are characterized by several principal bands. The band at 3650 cm^{-1} is attributed to alcoholic and phenolic, not hydrogen bonded –OH groups. In turn, the broad band centered at about 3400 cm^{-1} (Fig. 1a) is attributed to the stretching vibration of hydrogen-bonded hydroxyl groups. The band with the maximum at 3363 cm^{-1} suggests the presence of the OH-ether hydrogen bonds⁴. The band at about 3235 cm^{-1} is attributed to the “free” O-H groups of carboxylic acids³³ or ring C-H stretch of five-membered N/O-heterocycles such as furan and pyrrole¹². Decrease in the intensity of these bands (3500–3200 cm^{-1}) for biochar samples obtained in increasing pyrolysis temperatures indicates dehydration of cellulosic and ligneous components of the material¹². The band at about 3055 cm^{-1} , the most intensive in the FT-IR/PAS spectrum of BCW 500 sample, is associated with =C-H stretching mode of aromatic structures, which can be confirmed by the presence of relatively intense band at 1575 cm^{-1} and the presence of multiple bands within 960–700 cm^{-1} range (out-of-plane bending modes of aromatic structures)^{4, 12} (Fig. 1b). However, the band at ~3055 cm^{-1} may be the

Table 1. Physicochemical properties and elemental composition of BCW biochars

Biochar	C [%]	H [%]	N [%]	O [%]	H/C	O/C	(O+N)/C	Ash [%]	S_{BET} [m^2/g]	V_{micro} [cm^3/g]	S_{micro} [m^2/g]	pH
BCW 500	75.18	2.52	2.47	11.65	0.402	0.116	0.144	8.18	119.47	0.0470	95.54	10.18
BCW 600	79.50	1.96	1.93	9.53	0.296	0.090	0.111	7.09	34.87	0.0177	35.02	10.45
BCW 700	82.38	1.46	1.67	8.85	0.213	0.081	0.098	5.64	13.26	0.0086	17.01	11.39

S_{BET} – specific surface area, V_{micro} – volume of the micropores, S_{micro} – surface of the micropores

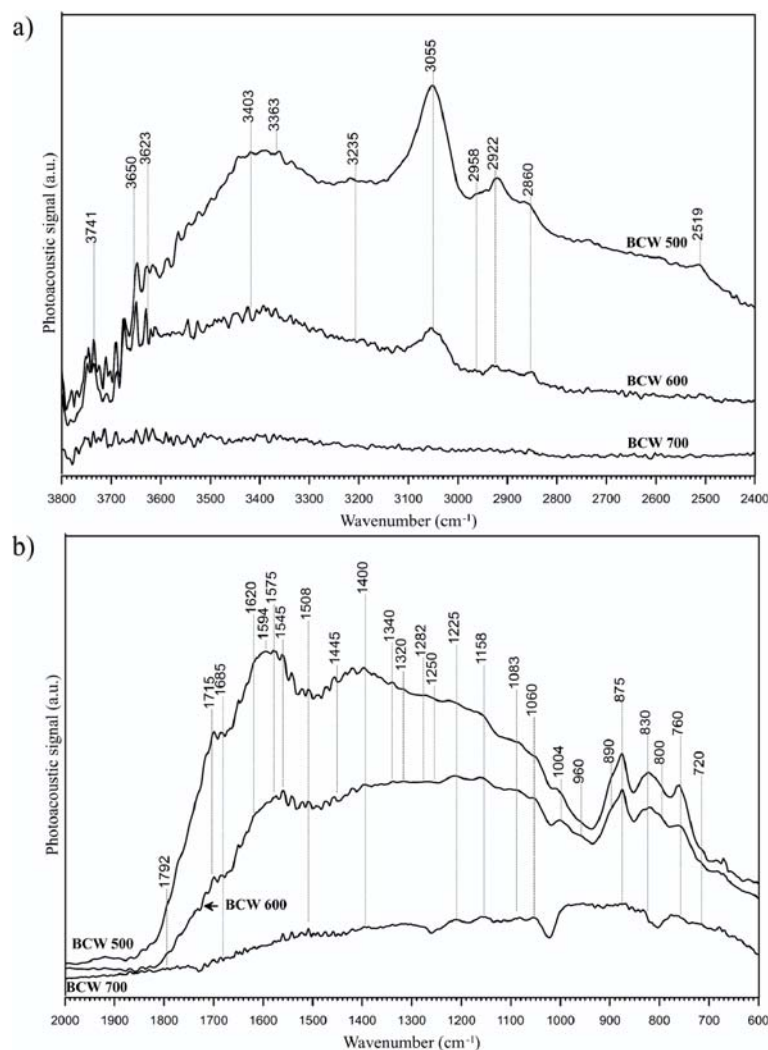


Figure 1. FT-IR/PAS spectra of BCW biochar samples in: a) 3800–2400 cm^{-1} range and b) 2000–600 cm^{-1} range

result of overlapping of both stretching mode of aromatic hydrocarbons and unsaturated aliphatic hydrocarbons³. Bands of aromatic hydrocarbons are present in the spectra of BCW 500 and BCW 600, but completely disappear in the BCW 700 spectrum. The bands of aliphatic C-H stretching, mostly methyl substituents of aromatic rings ($-\text{CH}_3$; 2958, 2860 cm^{-1}) and methylene linkages linking aromatic rings ($-\text{CH}_2-$; 2922, 2519 cm^{-1}), are present in the BCW 500 and BCW 600 spectra, but almost completely disappear in the BCW 700 spectrum. These results are consistent with the physicochemical data of examined biochars. Decrease in H/C ratio and hydrogen content in biochars with increasing pyrolysis temperature (Tab. 1) are in agreement with spectroscopic data.

The band within 1600–1580 cm^{-1} is often described by various authors, variously interpreted and still controversial. Some authors attribute it to vibration of C=O of lactones³⁴ or carboxyl-carbonate structures³⁵. Morterra et al.³⁶, performing isotope analysis, excluded the assignment of this band to carbonyl groups, and assigned it to C=C vibration in aromatic structures in the presence of oxygen structures. However, this band appears also in the spectra of samples which do not contain oxygen structures what may prove that its presence is connected more with C=C than C=O³⁴. Thus, the band at $\sim 1594 \text{ cm}^{-1}$ may be attributed both to C=C stretching in aromatic structures or C=O in carboxylates, ketones, quinones³⁶. As it was mentioned earlier, the bands at ~ 875 , 830 and 760 cm^{-1} correspond to aromatic C-H

out-of-plane deformation (more substituted rings appear at lower wavenumbers³). The band at $\sim 720 \text{ cm}^{-1}$ indicates the presence of long chain alkanes (CH_2 wagging). Loss of intensity of the bands at 1650–1500 cm^{-1} relative to that at 890–760 cm^{-1} , what is visible in Fig. 1b, proves the increase of the condensation degree for biochars obtained in elevated temperatures¹². The presence of C=O groups is confirmed by the shoulders at 1792, 1715 cm^{-1} (anhydride, ester) and 1685 cm^{-1} (aldehyde/ketone, carboxyl)³. The bands at 1508 and 1445 cm^{-1} are characteristic for aromatic skeletal vibrations, indicative for lignins. The vibrations between 1400 and 1050 cm^{-1} correspond to the presence of amide III, C-H, C-O, O-H in phenols and carboxylic acids or C-O-C in ethers, e.g. the bands of C-O-C groups and phenolic C-O of guaiacyl units associated with lignin at 1282 and 1250 cm^{-1} ¹². The decrease in the intensity of oxygen functional groups with increasing pyrolysis temperature is also the confirmation of changes in the physicochemical properties of biochars. Decrease in the amount of acidic groups can be confirmed by increasing pH of biochars and lowering of O/C and H/C ratio (Tab. 1). Bands responsible for C-H deformation and $-\text{C}=\text{C}-$ stretching in aromatic structures appear also within 1200–1000 cm^{-1} range. Additionally, the bands in the 1160–1000 cm^{-1} and 900–700 cm^{-1} range can be additionally assigned to vibrations of inorganic compounds in biochar, namely silica, carbonates, phosphates and nitrates (1083, 1060, 1004, 875, 830 cm^{-1})^{12, 37}. The sharp peak at $\sim 670 \text{ cm}^{-1}$

can be attributed to CO_2 , which is one of the products of pyrolysis and remains in the pores and/or is bound to the biochar surface strongly enough, that it cannot be removed under the measurement conditions. The origin of this band can also be due to the presence of atmospheric CO_2 . In the case of BCW 500 and BCW 600 spectra (Fig. 1) the relative intensity of the bands indicating the presence of aromatic and/or inorganic part of the biochar remained almost unchanged, while in the case of BCW 700 decreased significantly. The spectrum of BCW 700 revealed the loss of aromatic groups and the dominance of graphitic C^{38} .

In summary, differences in PAS spectra reflected water loss and depletion of organic matter (C-H, oxygen and nitrogen functional groups) that resulted from those heat-induced mass losses. The largest decrease in bands intensity occurred within $3500\text{--}3200\text{ cm}^{-1}$ and at 3055 cm^{-1} (aromatic compounds) and the latter completely disappeared in BCW 700 spectrum (Fig. 1a). The decrease in the bands intensity in photoacoustic spectra of the biochars samples produced with increasing pyrolysis temperature (Fig. 1) may be also caused by changes in density of these samples, since substances with bigger particle size generate lower photoacoustic signal²³. Along with the increase in the temperature of pyrolysis, there is a decrease in specific surface area, S_{BET} and micropores volume and surface (V_{micro} and S_{micro} , respectively – Ta-

ble 1). It can be related to decomposition and softening of some volatile fractions to form an intermediate melt in the char structure which can block the pores leading to decrease of biochar S_{BET}^{39} and formation of larger biochar particles.

Comparison of PAS, ATR, DRS and TS techniques

The most important thing when choosing a suitable IR technique is usefulness of the specific accessory for the particular application and thereby avoiding problems related to the specific technique. IR spectroscopy is a versatile tool for the study of biochar but the choice of the most suitable technique should be dictated by its simplicity, accuracy, reproducibility and possible nondestructivity, so that the sample can be used for other analyses. PAS, ATR and DRS used in this study were nondestructive, the samples were analyzed without time-consuming preparation. Since the IR technique should be simple and give reliable results, it would be also more convenient for the researcher not to perform complicated operations in order to find or induce bands.

Figures 2a and 2b show spectra of the same BCW 500 biochar sample, obtained using four different spectroscopic techniques (PAS, DRS, ATR, TS). All spectra were scaled and offset for clarity. The position of the corresponding peaks in the $3800\text{--}2400\text{ cm}^{-1}$ range is similar and within a few wavenumbers, although there

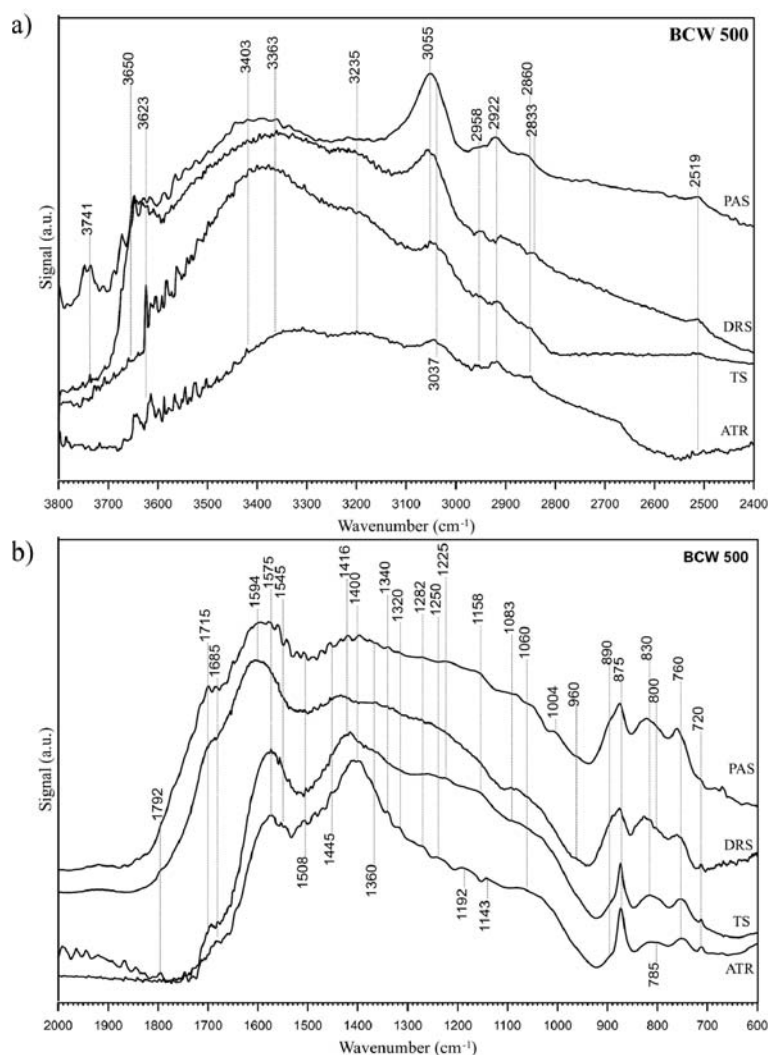


Figure 2. Comparison of PAS, DRS, ATR and TS spectra of BCW 500 biochar sample in: a) $3800\text{--}2400\text{ cm}^{-1}$ range and b) $2000\text{--}600\text{ cm}^{-1}$ range

are slight differences regarding the intensities of the individual bands. The difference between all the spectra in Fig. 2a are particularly noticeable while considering the intensity of the band of hydrogen-bonded hydroxyl groups ($\sim 3400\text{ cm}^{-1}$), which is the most intense in TS spectrum of BCW 500. In all spectra in Fig. 2a the $=\text{C-H}$ band of stretching mode of aromatic structures ($\sim 3055\text{ cm}^{-1}$) is well resolved and have similar intensity.

The position and intensity of C-H bands ($2960\text{--}2830\text{ cm}^{-1}$) also display a similar trend in DRS, ATR and PAS spectra, although those peaks are the most intense in PAS spectrum of BCW 500 and have the lowest intensity in TS spectrum (Fig. 2a). In the case of TS spectrum this is most likely due to the fact that the largest number of these groups is on the surface of biochar sample, and TS detects the bulk of the biochar and is unable to identify the oxidation in the near-surface region. Thus, PAS and ATR appear to be the most appropriate techniques to observe $3600\text{--}2400\text{ cm}^{-1}$ spectral range.

Making the ATR spectrum may sometimes cause some difficulties, because biochar samples may display negative peaks in ATR measurements²², especially in $3800\text{--}2400\text{ cm}^{-1}$ region, what consequently interfere with the interpretation of the ATR spectra. The appearance of negative peaks is most commonly caused by the contamination of the ATR crystal, atmospheric water, carbon dioxide or

residual solvent in the atmosphere while collecting the background immediately after cleaning the ATR crystal.

The differences in the spectral response are visible also in the $2000\text{--}600\text{ cm}^{-1}$ region (Fig 2b). As in the previous region, in the $2000\text{--}600\text{ cm}^{-1}$ range DRS, ATR and PAS spectra are similar to one another, although there are some bands present only in PAS spectrum. The bands not visible in the DRS spectrum, however, are present in the spectrum made using ATR technique and, to a lesser extent, in TS spectrum. Analyzing the spectra in Fig. 2b it can be concluded that PAS and ATR techniques are in this case the most suitable for analysis of oxygen groups on biochar, especially in the $1400\text{--}1000\text{ cm}^{-1}$ range. Those bands are well resolved, while in DRS and TS spectra they are almost invisible, present mainly as a shoulders.

Analyzing all IR spectra of BCW 600 biochar sample in Fig. 3b, a significant decrease in the number of oxygen functional groups relative to BCW 500 biochar spectra (Fig. 2b) is noticeable, while the intensity of the bands responsible for the aromatic and/or inorganic part in biochar remained practically unchanged, both in $3800\text{--}2400\text{ cm}^{-1}$ (Fig. 3a) and $2000\text{--}600\text{ cm}^{-1}$ range (Fig. 3b). In all presented spectra bands of aromatic hydrocarbons at $\sim 3055\text{ cm}^{-1}$ are visible (Fig. 3a). The bands of C-H groups are visible and well resolved only in the PAS and ATR spectra of BCW 600 biochar while in the spectra

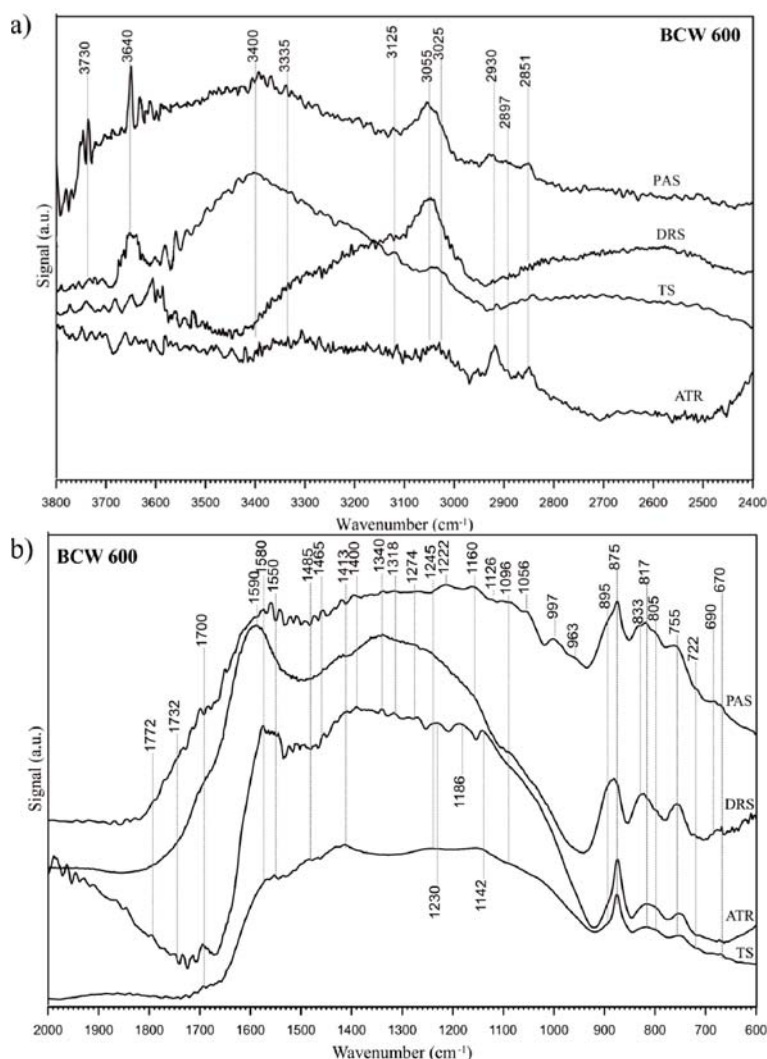


Figure 3. Comparison of PAS, DRS, ATR and TS spectra of BCW 600 biochar sample in: a) $3800\text{--}2400\text{ cm}^{-1}$ range and b) $2000\text{--}600\text{ cm}^{-1}$ range

obtained using two other techniques those bands have very low intensity. In the fingerprint region the spectral features are the most similar in the PAS and ATR spectra, while in DRS and TS spectra bands of oxygen groups are poorly visible. The intensity of the bands within 900–700 cm^{-1} remains substantially unchanged while compared to BCW 500 spectra showed in Fig. 2b.

Analyzing all the spectra of BCW samples in the fingerprint region (Fig. 2b, 3b, 4b) it can be seen that the higher the pyrolysis temperature, the differences in the shape and position of each band in the spectra obtained with different IR techniques are more visible. This is particularly noticeable in the BCW 700 spectra (Fig. 4b). Although the position of the bands is almost identical, the intensities of the bands vary considerably. The band at $\sim 1580 \text{ cm}^{-1}$ is a shoulder in the case of PAS and ATR spectra, while in DRS and TS spectra it is a well resolved peak. In turn, in ATR and TS spectra this peak is shifted to lower wavenumbers ($\sim 1556 \text{ cm}^{-1}$). The band at $\sim 1455 \text{ cm}^{-1}$ is visible in the PAS, DRS and TS spectra as a shoulder, but in the case of ATR spectrum it is a broad, but well resolved band, indicating the presence of aromatic C=C stretching. The band at

872 cm^{-1} in ATR spectrum also indicates the presence of aromatic groups and is particularly well visible in this spectrum (Fig. 4b). In the case of PAS and TS spectra this peak has low intensity, whereas in the DRS spectrum is split into two bands at 900 and 840 cm^{-1} . The peak within 1340–1315 cm^{-1} (combination band of phenolic OH deformation vibrations, C-O stretching and C-N stretching in aromatic amines) is in turn intensive in DRS spectrum, while in the case of other spectra appears as a shoulder. The band at $\sim 1096 \text{ cm}^{-1}$ (C-O-C, C-OH) is also visible in all the spectra, but is particularly well pronounced in DRS and TS spectra. Practically no peaks were observed in all the spectra of BCW 700 in 3800–2400 cm^{-1} range (Fig. 4a).

Spectral line shapes are affected by many factors. Some of the spectra presented in this study have substantial noise, regardless of the technique used, resulting from the presence of moisture and/or the use of relatively high resolution (4 cm^{-1}). Moisture in the samples is present even after long drying (72–120 h, 105°C). The spectra were intentionally not smoothed, because smoothing decreases spectral resolution and some bands with low intensity might be erased. The resolution is also one

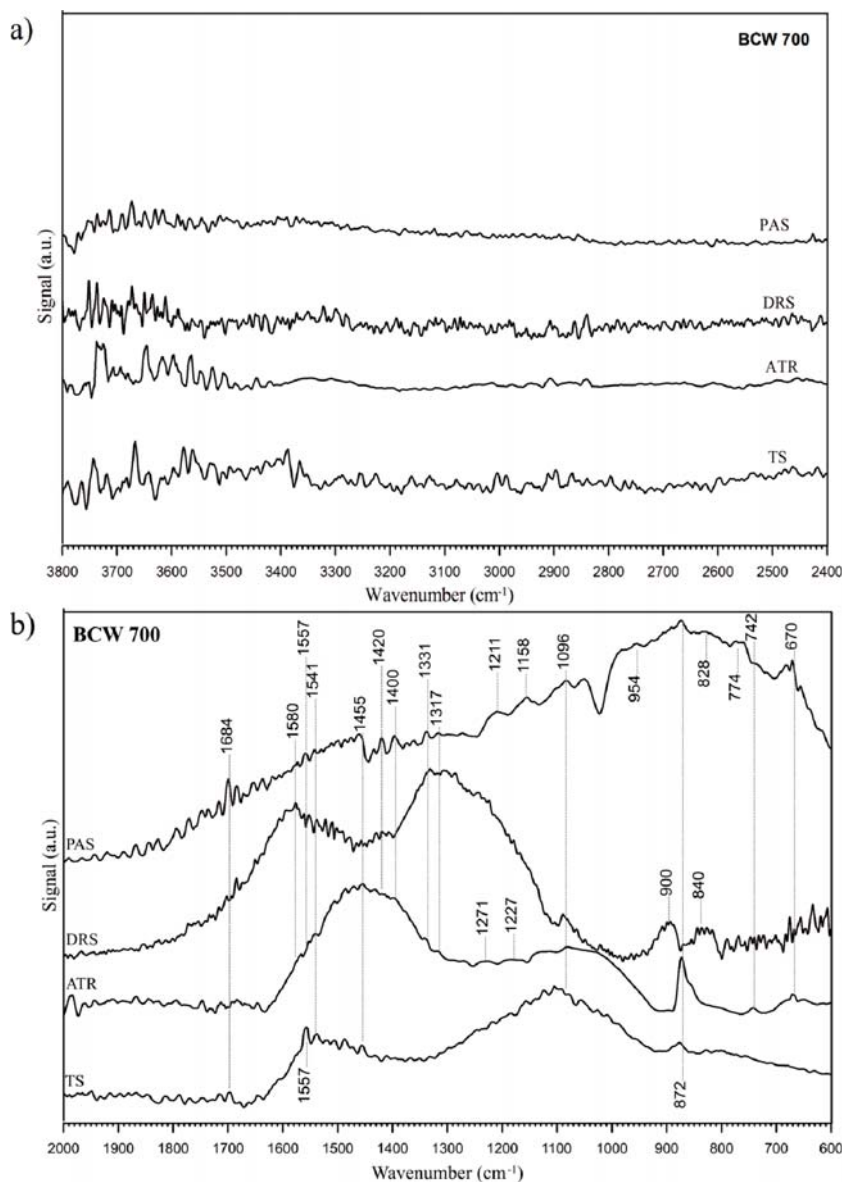


Figure 4. Comparison of PAS, DRS, ATR and TS spectra of BCW 700 biochar sample in: a) 3800–2400 cm^{-1} range and b) 2000–600 cm^{-1} range

of the parameters involved in obtaining FT-IR spectra. Application of higher resolution reveals the fine spectral features, but extends the data acquisition time and sometimes makes spectra noisy.

IR spectroscopic analysis allowed to observe changes on the biochar surface depending on the pyrolysis temperature. The results of conducted analysis showed that the physicochemical properties of biochars are strongly influenced by the temperature of pyrolysis. Increase in the pyrolysis temperature increased the carbon content, decrease in hydrogen, nitrogen and oxygen content. The loss of oxygen groups and aliphatic part of the biochar has been confirmed using different IR spectroscopy techniques.

CONCLUSIONS

This study shows the effectiveness and usefulness of four different FT-IR spectroscopic techniques in rapid and, in the case of PAS, ATR and DRS, non-destructive direct measurement of the biochars formation in different pyrolysis temperatures. These techniques provide fundamental information on biochar composition and surface properties. The comparison of the spectra obtained by the four FT-IR techniques allows to conclude that although some differences are observed between the corresponding spectra, any of these techniques can be used as efficient tool to control biochar's surface functional groups quality. Nevertheless, PAS and ATR seem to be the best techniques of the four, since they require hardly any sample preparation, simultaneously providing good quality spectra of biochars.

The studies presented in this paper are consistent with similar comparisons of IR techniques made for biomass samples²⁸, where it was found that ATR was the best technique in order to obtain smooth spectra with easily distinguished peaks, in contrast to transmission spectroscopy, where the spectra had less specific peaks and separation of the bands was worse. Furthermore, preparation of the samples for TS measurements is laborious, time consuming and suffers from risk of samples contamination. These factors and often unsatisfactory appearance of the spectra are not an indication for the routine measurements in biochar analysis. Additionally, due to the manner of sample's preparation, TS allows to detect mainly the features of sample's bulk and is not suitable for testing the surface, which is particularly important while studying functional groups on the biochar surface.

The DRS technique turned out to be the weakest, due to poor spectral quality and poor separation of the bands. Additionally, as it was mentioned before, the same sample may give different spectra in different DRS experiments, because the reflectance intensity is influenced by the sample preparation, what makes any attempts to quantify the spectra difficult. In the case of the studies presented in this work, PAS and ATR turned out to be the best of all four spectroscopic techniques for biochar analysis. Research carried out in this work and literature reports²⁸ indicate that the PAS and ATR techniques, with the ability to distinguish functional groups, appeared to be the most appropriate when choosing the most reliable technique for spectral quantification.

Apart from the above conclusions, due to the differences in the position and intensity of the bands in the spectra obtained using four different IR spectroscopy techniques (PAS, ATR, DRS, TS), in order to acquire consistent and accurate spectroscopic data, one selected spectroscopic technique should be used consequently. This will prevent inconsistencies while comparing the spectra of biochars made in different conditions.

ACKNOWLEDGEMENTS

This study was supported by the grant from Switzerland through the Swiss Contribution to the enlarged European Union.

LITERATURE CITED

1. Tag, A.T., Duman, G., Ucar, S. & Yanik, J. (2016). Effects of feedstock type and pyrolysis temperature on potential applications of biochar. *J. Anal. Appl. Pyrol.* 120, 200–206. DOI: 10.1016/j.jaap.2016.05.006.
2. Lehmann, J., Czimczik, C., Laird, D. & Sohi, S. (2009). Stability of biochar in soil, In *Biochar for Environmental Management: Science and Technology*; Lehmann, J., Stephen, J., Eds.; Earthscan Publ.: London, 183–205.
3. Yang, C.Q., Simms, J.R. (1995). Comparison of photoacoustic, diffuse reflectance and transmission infrared spectroscopy for the study of carbon fibers. *Fuel* 74, 543–548. DOI: 10.1016/0016-2361(95)98357-K.
4. Gomez-Serrano, V., Piriz-Almeida, F., Duran-Valle, C.J. & Pastor-Villegas, J. (1999) Formation of oxygen structures by air activation. A study by FT-IR spectroscopy. *Carbon* 37, 1517–1528. DOI: 10.1016/S0008-6223(99)00025-1.
5. Yarwood, J. (1993). Fourier Transform Infrared Reflection Spectroscopy for surface analysis *Analytical Proceedings, Surface Analysis* 30, 13–18.
6. Kim, K.H., Kim, J.Y., Cho, T.S. & Choi, J.W. (2012). Influence of pyrolysis temperature on physicochemical properties of biochar obtained from the fast pyrolysis of pitch pine (*Pinus rigida*). *Bioresource Technol.* 118, 158–162. DOI: 10.1016/j.biortech.2012.04.094.
7. Ghani, W.A.K., Azlina, W. & Da Silva, G. (2014). Sawdust-derived biochar: Characterization and CO₂ adsorption/desorption study. *J. Appl. Sci.* 14, 1450–1454. DOI: 10.3923/jas.2014.1450.1454.
8. Mukome, F.N.D., Zhang, X., Silva, L.C.R., Six, J. & Parikh, S.J. (2013). Use of chemical and physical characteristics to investigate trends in biochar feedstock. *J. Agric. Food Chem.* 61, 2196–2204. DOI: 10.1021/jf3049142.
9. Mašek, O., Budarin, V., Gronnow, M., Crombie, K. & Brownsort, P. (2013). Microwave and slow pyrolysis biochar – comparison of physical and functional properties. *J. Anal. Appl. Pyrolysis* 100, 41–48. DOI: 10.1016/j.jaap.2012.11.015.
10. Cantrell, K.B., Hunt, P.G., Uchimiya, M., Novak, J.M. & Ro, K.S. (2012). Impact of pyrolysis temperature and manure source on physicochemical characteristics of biochar. *Bioresource Technol.* 107, 419–428. DOI: 10.1016/j.biortech.2011.11.084.
11. Liu, Y., He, Z. & Uchimiya, M. (2015). Comparison of biochar formation from various agricultural by-products using FTIR spectroscopy. *Modern Appl. Sci.* 9, 246–253. DOI: 10.5539/mas.v9n4p246.
12. Kieluweit, M., Nico, P.S., Johnson, M.G. & Kleber, M. (2010). Dynamic molecular structure of plant biomass-derived black carbon (biochar). *Environ. Sci. & Technol.* 44, 1247–1253. DOI: 10.1021/es9031419.
13. Chia, C.H., Gong, B., Joseph, S.D., Marjo, C.E., Munroe P. & Rich A.M. (2012). Imaging of mineral-enriched biochar

by FTIR, Raman and SEM-EDX. *Vibrational Spectroscopy* 62, 248–257. DOI: 10.1016/j.vibspec.2012.06.006.

14. Al-Wabel, M.I., Al-Omran, A., El-Naggar, A.H. & Nadeem, M. (2013). Pyrolysis temperature induces changes in characteristics and chemical composition of biochar produced from conocarpus wastes. *Bioresource Technol.* 131, 374–379. DOI: 10.1016/j.biortech.2012.12.165.

15. Abdulrazaq, H., Jol, H., Husni, A. & Abu-Bakr, R. (2014). Characterization and stabilization of biochar obtained from empty fruit bunch, wood and rice husk. *BioResources* 9, 2888–2898. DOI: 10.15376/biores.9.2.2888-2898.

16. Angin, D. (2013). Effect of pyrolysis temperature and heating rate on biochar obtained from pyrolysis of safflower seed press cake. *Bioresource Technol.* 128, 593–597. DOI: 10.1016/j.biortech.2012.10.150.

17. Jung, K.W., Jeong, T.U., Kang, H.J., Ahn, K.H. (2016). Characteristics of biochar derived from marine macroalgae and fabrication of granular biochar by entrapment in calcium-alginate beads for phosphate removal from aqueous solution. *Bioresource Technol.* 211, 108–116. DOI: 10.1016/j.biortech.2016.03.066.

18. Qiu, Y., Cheng, H., Xu, C. & Sheng, G.D. (2008). Surface characteristics of crop-residue-derived black carbon and lead(II) adsorption. *Water Research* 42, 567–574. DOI: 10.1016/j.watres.2007.07.051.

19. Jindo, K., Mizumoto, H., Sawada, Y., Sanchez-Monedero, M.A. & Sonoki, T. (2014). Physical and chemical characterization of biochars derived from different agricultural residues. *Biogeosciences* 11, 6613–6621. DOI: 10.5194/bgd-11-11727-2014.

20. Harris, K., Gaskin, J., Cabrera, M., Miller, W. & Das, K.C. (2013). Characterization and mineralization rates of low temperature peanut hull and pine chip biochars. *Agronomy* 3 (2), 294–312. DOI: 10.3390/agronomy3020294.

21. Wang, C., Tu, Q., Dong, D., Strong, P.J., Wang, H., Sun, B. & Wu, W. (2014). Spectroscopic evidence for biochar amendment promoting humic acid synthesis and intensifying humification during composting. *J. Hazard. Mater.* 280, 409–416. DOI: 10.1016/j.jhazmat.2014.08.030.

22. Cao, X. & Harris, W. (2010). Properties of dairy-manure-derived biochar pertinent to its potential use in remediation. *Bioresource Technol.* 101, 5222–5228. DOI: 10.1016/j.biortech.2010.02.052.

23. Michaelian, K.H. (2010). *Photoacoustic IR spectroscopy*, 2nd Ed., Wiley-VCH Verlag GMBH&Co.

24. Brewer, C.E., Schmidt-Rohr, K., Satrio, J.A. & Brown, R.C. (2009). Characterization of biochar from fast pyrolysis and gasification systems. *Environmental Progress & Sustainable Energy* 28, 386–396. DOI: 10.1002/ep.10378.

25. Yuan, J.H., Xu, R.K. & Zhang, H. (2011). The forms of alkalis in the biochar produced from crop residues at different temperatures. *Bioresource Technol.* 102, 3488–3497. DOI: 10.1016/j.biortech.2010.11.018.

26. Oleszczuk, P., Joško, I., Futa, B., Pasieczna-Patkowska, S., Pałys, E. & Kraska, P. (2014). Effect of pesticides on microorganisms, enzymatic activity and plant in biochar-amended soil. *Geoderma* 214–215, 10–18. DOI: 10.1016/j.geoderma.2013.10.010.

27. Zielińska, A., Oleszczuk, P., Charnas, B., Skubiszewska-Zięba, J. & Pasieczna-Patkowska, S. (2015). Effect of sewage sludge properties on the biochar characteristics. *J. Anal. Appl. Pyrolysis* 112, 201–213. DOI: 10.1016/j.jaap.2015.01.025.

28. Gogna, M. & Goacher, R.E. (2018). Comparison of three Fourier transform infrared spectroscopy sampling techniques for distinction between lignocellulose samples. *BioResources* 13(1), 846–860. DOI: 10.15376/biores.13.1.846-860.

29. Faix, O. & Böttcher, J.H. (1992). The influence of particle size and concentration in transmission and diffuse reflectance spectroscopy of wood. *Holz als Roh- und Werkstoff* 50(6), 221–226. DOI: 10.1007/BF02650312.

30. Zielińska, A. & Oleszczuk, P. (2015). The conversion of sewage sludge into biochar reduces polycyclic aromatic hydrocarbon content and ecotoxicity but increases trace metal content. *Biomass & Bioenergy* 75, 235–244. DOI: 10.1016/j.biombioe.2015.02.019.

31. Novak, J.M., Lima, I., Xing, B., Gaskin, J.W., Steiner, C., Das, K.C., Ahmedna, M., Rehrah, D., Watts, D.W., Busscher, W.J. & Schomberg, H. (2009). Characterization of designer biochar produced at different temperatures and their effects on a loamy sand. *Annals Environ. Sci.* 3, 195–206.

32. Gregg, S.J. & Sing, K.S.W. (1982). *Adsorption, Surface Area and Porosity*, Academic Press, London.

33. Qui, Y. & Ling, F. (2006). Role of surface functionality in the adsorption of anionic dyes on modified polymeric sorbents. *Chemosphere* 64, 963–971. DOI: 10.1016/j.chemosphere.2006.01.003.

34. Zawadzki, J. (1989). *Infrared Spectroscopy in Surface Chemistry of Carbons*, in: *Chemistry and Physics of Carbon*, Vol. 21, Thrower, P.A., Ed.; Dekker: New York.

35. Morterra, C. & Low, M.J.D. (1982). The nature of the 1600 cm⁻¹ band of carbons. *Spectroscopy Letters* 15, 689–697.

36. Morterra, C., O'Shea, M.L., Low, M.J.D. (1988). Infrared studies of carbons – IX. The vacuum pyrolysis of non-oxygen-containing materials: PVC. *Materials Chemistry and Physics* 20, 123–144.

37. Chukanov, N.V. (2014). *Infrared spectra of mineral species*, Extended Library, Vol. 1, Springer.

38. Bourke, J., Manley-Harris, M., Fushimi, C., Dowaki, K., Nunoura, T. & Antal, M.J. (2007). Do all carbonized charcoals have the same chemical structure? 2. A model of the chemical structure of carbonized Charcoal. *Industrial Engin. Chem. Res.* 46, 5954–5967. DOI: 10.1021/ie070415u.

39. Lua, A.C., Yang, T. & Guo, J. (2004). Effects of pyrolysis conditions on the properties of activated carbons prepared from pistachio-nut shells. *J. Anal. Appl. Pyrolysis* 72, 279–287. DOI: 10.1016/j.jaap.2004.08.001.